Deep-Learning-based MR Compressed Sensing using Non-randomly Under-sampled Signal in Nonlinear Phase Encoding Imaging

Satoshi ITO* and Shohei OUCHI*
* Graduate Program in Information, Electrical and Electronic Systems Engineering
Graduate School of Regional Development and Creativity
Utsunomiya University, Tochigi, Japan
E-mail: itohst@is.utsunomiya-u.ac.jp Tel/Fax: +81-286-6896276

***Abstract*—Optional image scaling, and hence aliasless image reconstruction, is feasible using a signal that violates the sampling theorem in MR phase scrambling Fourier transform imaging. In this method, the main and aliased image components are separated in the scaled space when a large scaling factor is selected. In the present study, a new fast imaging method, in which aliasing artifacts caused by undersampling of the signal, are removed in two steps: in the downscaled space introduced by aliasless reconstruction and through de-aliasing using a deep convolution neural network. The proposed method is shown to provide higher PSNR images compared to random sampling compressed sensing and has an advantage in terms of low-sampling-rate image acquisition.**

I. Introduction

Magnetic resonance imaging (MRI) requires a long scan time, which is much longer than that of X-ray CT, and, to date, numerous techniques have been proposed in order to speed up the scan time. The recent theory of compressed sensing (CS)[1], [2] may reduce the number of measurements required for MR imaging (CS-MRI)[3]. In recent years, the deep convolutional neural network (CNN) has received a great deal of attention because of its excellent performance in the field of CS image reconstruction. The first application of CNN to MR imaging was de-aliasing of alias-superimposed images obtained in parallel imaging, which is classified as image domain learning[4]. Lee et al. proposed a deep learning network for the reconstruction of MR images in which the multi-scale network structure called U-Net is used to cope with globally distributed artifact patterns and phase image reconstruction[5].

In contrast to image domain learning, there is also k-space learning, such as in AUTOMAP software [6], in which transformation from the source signal (k-space signal) to the target image domain can be obtained by data-driven supervised learning. Images can be reconstructed directly from the under-sampled k-space signal with AUTOMAP. However, the practicality of AUTOMAP remains limited because the required number of parameters scales quadratically with the input size. Therefore, training in the image domain is beneficial and practical in the sense that fewer parameters facilitate training and are less prone to overfitting. In the present paper, we propose an imaged-domain-based CS reconstruction method, in which equi-spaced undersampling is adopted and aliasing artifacts are removed by aliasing control in the scaled space introduced by alias-less reconstruction, followed by a deep convolutional neural network.

We have proposed a new image reconstruction technique, in which images at optional scaling can be obtained and hence aliasless images can be reproduced from the data containing aliasing artifacts in the Fourier transform image reconstruction technique [7], [8]. Since an aliasless image is realized by expanding the pseudo FOV, the spatial resolution of that image must be reduced. In the present study, aliasless image reconstruction is used to scale the main image components and the aliased image components in the highly downscaled image domain. The advantage of the proposed method is that most aliasing artifacts are removed in this downscaled image domain and, therefore, it is easier for the CNN to learn and remove the remaining small artifacts. In order to clarify the characteristics of the proposed two-step hybrid reconstruction, it was compared with image domain CNN and ADMM CS-net[9], which is a kind of k-space learning method and conventional iterative reconstruction.

II. Phase Scrambling Fourier Imaging

Phase-scrambling Fourier transform (PSFT) imaging is a technique whereby a quadratic field gradient $\Delta B = b(x^2+y^2)$ is added to the pulse sequence of conventional FT imaging in synchronization with the field gradient for phase encoding [10], [11]. The signal obtained in PSFT is given as:

$$v(k_x,k_y)=\iint_{-\infty}^{\infty}\left\{\rho(x,y)e^{-j\gamma b\tau(x^2+y^2)}\right\}e^{-j(k_xx+k_yy)}dxdy \quad (1)$$

where $\rho(x,y)$ represents the spin density distribution in the subject, γ is the magnetogyric ratio, and b and τ are the coefficient and impressing time, respectively, of the quadratic field gradient. Equation (1) can be rewritten as the Fresnel transform equation using the variable substitutions $x' = k_x/2\gamma b\tau$ and

$y' = k_y/2\gamma b\tau$, as follows:

$$\begin{aligned} & v(x',y')e^{-j\gamma b\tau(x'^2+y'^2)} \\ &\quad = \iint_{-\infty}^{\infty} \rho(x,y) e^{-j\gamma b\tau\left\{(x'-x)^2+(y'-y)^2\right\}} dxdy \quad (2) \\ &\quad = \rho(x,y) * e^{-j\gamma b\tau(x^2+y^2)} = v_{FR}(x',y') \quad (3) \end{aligned}$$

The right-hand side of Eq. (2) is known as the Fresnel transform equation, which is familiar in optics or sound wave analysis [12]. Magnetic resonance imaging imposing the quadratic phase on the subjects, also referred to as nonlinear encoding, has attracted attention in recent years because of its flexible image processing and unique features[13], [14], [15].

III. Alias-less Image Reconstruction

Object images can be obtained by inverse Fresnel transform from a signal described by Eq. (2) [7]. Reconstruction involves 1) multiplying a quadratic phase term numerically by the signal in the PSFT in order to obtain the signal shown in Eqs. (1) and (2), solving $\rho(x,y)$ using the inverse filtering technique, as follows:

$$\rho(x,y) = \frac{\gamma b\tau}{\pi} e^{j\frac{\pi}{2}} \mathcal{F}^{-1}\left[e^{j\frac{\omega_x^2+\omega_y^2}{4\gamma b\tau}} \mathcal{F}\left[v_{FR}(x',y')\right]\right] \quad (4)$$

The imaging parameter $\gamma b\tau$, which is the coefficient of quadratic phase modulation, is necessary for image reconstruction as shown in Eq. (4). The spatial resolution of reconstructed images is almost the same as the signal step of the Fresnel transformed signal:

$$\Delta x' = \frac{\pi}{\gamma b\tau N\Delta x}, \qquad \Delta y' = \frac{\pi}{\gamma b\tau N\Delta y} \quad (5)$$

Suppose the parameter $\alpha\gamma b\tau$ is used in place of the true $\gamma b\tau$ obtained experimentally in the Fresnel reconstruction equations and substituting the variables $u = x/\alpha$ and $v = y/\alpha$. Then, the Fresnel transformed signal v_α is written as follows:

$$v_\alpha(x',y') = \iint_{-\infty}^{\infty} s(u,w) e^{-j\alpha\gamma b\tau\left\{(x'-u)^2+(y'-w)^2\right\}} dudw \quad (6)$$

$$s(u,w) = \alpha^2 \rho(\alpha u,\alpha w) e^{-j\left(\frac{\alpha-1}{\alpha}\right)\gamma b\tau\left\{(\alpha u)^2+(\alpha w)^2\right\}} \quad (7)$$

We can obtain image function $\rho(x,y)$ by Eq.(6) as,

$$\rho(\alpha u,\alpha w) = \frac{1}{\alpha^2} s(u,w) e^{j\left(\frac{\alpha-1}{\alpha}\right)\gamma b\tau\left\{(\alpha u)^2+(\alpha w)^2\right\}} \quad (8)$$

The reconstructed image is scaled by a factor of α. Since α is given in the reconstruction procedure, we can set an optional scale to the reconstructed image as α. Consider the case in which an aliasing artifact occurs in the Fourier-reconstructed image using the PSFT signal. Fresnel reconstruction by Eq. (7) then offers an aliasless image reconstruction (ALR) by shrinking the image using an adequate scaling parameter α, so as to appear smaller than the FOV.

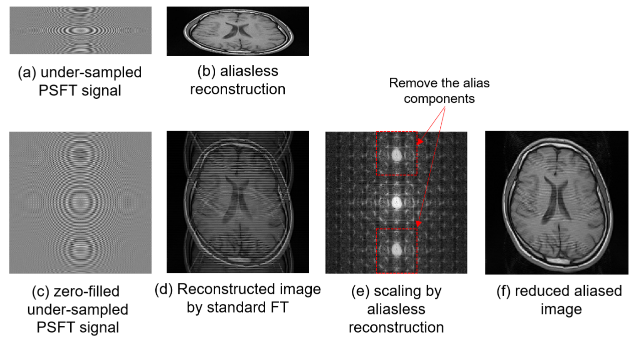

Fig. 1. Removal of aliasing components using aliasless image reconstruction. (a) Undersampled phase-scrambling Fourier transform (PSFT) signal and (b) aliasless images by aliasless image reconstruction (ALR). Spatial resolution is reduced. (d) Fourier transform image using the zero-filled PSFT signal. (e) Aliasless image reconstruction image with high downscaling factor. (f) After removing the main aliased image components (red square box), a nearly aliasless image can be obtained.

IV. De-aliasing by aliasless image reconstruction and convolutional neural network

Figure 1 shows the proposed method. As shown in Fig. 1(a), an aliasless image can be reconstructed using a regularly undersampled PSFT signal. However, the spatial resolution is reduced according to the number of sampled points, as shown in Fig. 1(b). Figure 1(c) shows the zero-filled PSFT signal, where zero-datum are filled in the skipped sampling points, and the reconstructed image applying inverse Fourier transform to the signal. Serious fold-over artifacts appear on the reconstructed image. Figure 1(e) shows the ALR images with high downscale factor α. Since the optional value can be chosen for the scaling factor α in the image reconstruction process irrespective of the actual parameter used in the data acquisition, images can be reconstructed, as shown in Fig. 1(e). When ALR is executed with a high downscaling factor using a zero-filled undersampled signal, the main image components and aliasing components will be separated in the scaled space, as shown in Fig. 1(e). After removing the main aliasing components indicated by the red boxes and applying inverse ALR, almost all aliasing artifacts are removed from the reconstructed image, as shown in Fig. 1(f). Note that, in proposed method, the manner of signal undersampling is equally spaced skipping, which is not usually adopted in standard Fourier-transform-based imaging, because it is impossible to separate the main image and aliasing image components, in general. Therefore, a high signal reduction factor is expected in proposed method.

Since some aliasing artifacts are remained in the reduced aliased image, a deep convolutional neural network (CNN) is adopted in order to remove the remaining artifacts. We used a deep CNN, which is known to have high de-aliasing performance without sacrificing spatial resolution, inspired by Zhang's denoising CNN (DnCNN) [16]. The structure of the

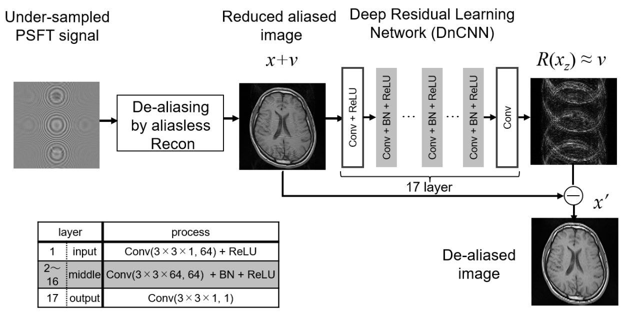

Fig. 2. Deep convolutional neural network (CNN) used for removing the remaining artifacts.
The input of CNN is the reduced alias image $x_z = x + v$, where x is the target image, and v are the remaining artifacts on the image. The CNN learns and estimates the remaining artifacts v on the image (b).

deep CNN is shown in Fig. 2. Letting aliasing artifacts v remain on image x, reduced alias image x_z can be expressed as $x_z = x + v$. When the original mapping is more like an identity mapping, the residual mapping will be much easier to optimize [19]. Image x_z is much more like the fully scanned image x and close to identity mapping. Therefore, residual learning formulation is more suitable for image de-aliasing. Letting $R(x_z)$ be the residual mapping to predict v ($R(x_z) \approx v$), reconstructed image x' is obtained by $x' = x_z - R(x_z)$. The loss function used to update the network parameter is the mean squared error between the true and estimated artifacts. Figure 2 shows the network structure used in the present study.

V. Experiments

The structure of the CNN is as follows. The receptive field size is 35, and the network has 17 layers. The filter size is 3 x 3 x 64. Adam was used for the optimizer, and the batch size of the input dataset is 128. In de-aliasing MR images, the size of output image should be the same as the input aliased image. Therefore, simple zero data padding is carried out at the boundary before the Conv operation, so that the feature map of the middle layers has the same size as the input image. A total of 100 images were used for the learning of the deep CNN network. In simulation experiments, the PSFT signal is calculated using the MR healthy volunteer image data according to Eq. (1). Calculated signals were undersampled at an equal interval at acceleration factors of 2x, 3x, and 4x. The imaging parameters are set to be $\alpha_{true} = 1.0$ for data acquisition, and α for reconstruction is 0.125, 0.083, or 0.0625. Figures 3(a), 3(b), and 3(c) are downscaled images using aliasless reconstruction for acceleration factor 2x, 3x, and 4x, respectively. Most of the aliasing artifacts were removed by removing these separated aliased components surrounded by the red dashed lines. The parameter α and the dimensions of the red dashed lines in Figs. 3(a), 3(b), and 3(c) were determined by preliminary reconstruction experiments. The obtained reduced aliased images are shown in Figs. 3(d), 3(e), and 3(f) and were used as the input images of the deep CNN. The output images by the CNN are shown in Figs. 3(g), 3(h), and 3(i). Figures 3(j), 3(k), and 3(l) are the residuals of output images (g), (h), and (i). As shown in (g), (h), and (i), the remaining artifacts are clearly removed by the deep CNN network without conspicuous degradation of the spatial resolution. Figure 4 shows the PNSR characteristics with reference to the signal reduction factor using 20 phase varied images. The proposed method is compared with a simple image domain learning CNN using the network shown in Fig. 1 and ADMM-CSnet[9], as well as CS iterative reconstruction using the PSFT signal (PSFT-CS) [17]. Random undersampling was used, except in the proposed method. Figure 4 indicates that the proposed method shows a higher PSNR, especially for lower sampling rates of 25% and 33%.

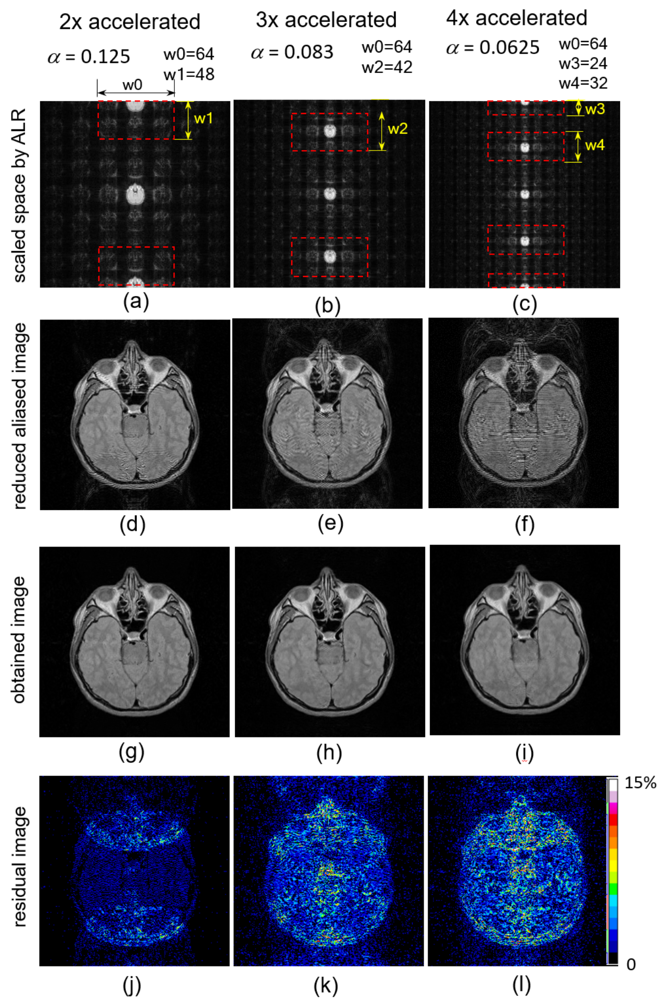

Fig. 3. Results of reconstruction experiments.
(a), (b), and (c) Scaled images by ALR for acceleration factors of 2x, 3x, and 4x, respectively. (d), (e), and (f) Reduced aliased images obtained by removing the red rectangular region. (g), (h), and (i) Obtained images. (j), (k), and (l) Residuals of images (g), (h), and (i), respectively.

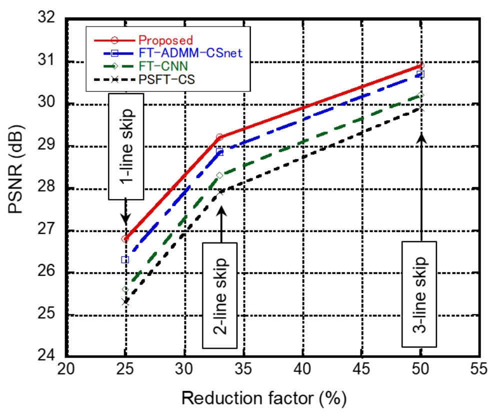

Fig. 4. Comparison of PSNR with PSFT compressed sensing and Fourier transform compressed sensing with reference to signal reduction factor.

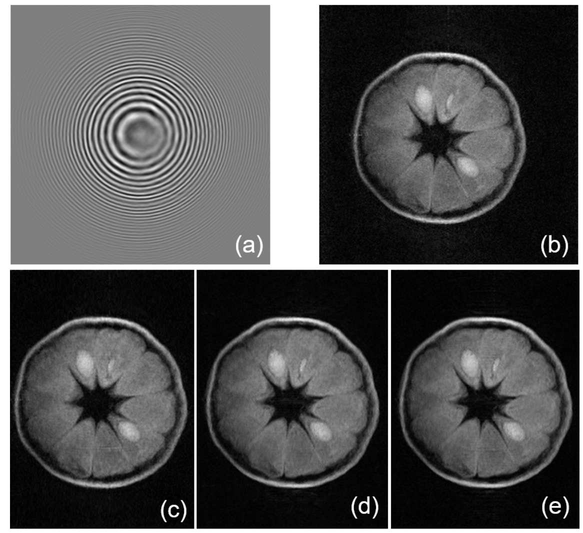

Fig. 5. Reconstructed images using the experimentally obtained PSFT signal. (a) Obtained PSFT signal using 0.2 T handmade MRI, (b) fully scanned (256 x 256) images, and (c), (d), and (e) obtained images for acceleration factors of 2x, 3x, and 4x, respectively. Although slight residuals of artifacts were observed, images with good resolution were obtained.

Figure 5 shows the results of application to the experimentally obtained PSFT signal. The quadratic field gradient $b(x^2 + y^2)$ required to realize the PSFT was generated by a coil designed for line-scan imaging. Fully scanned signal imaging shown in Fig. 5(a) was acquired using 0.2T MRI, and then the obtained signal was undersampled in the phase encoding direction in a computer. The imaging parameters are N=256, $\gamma b\tau$=1.53 $\mathrm{rad/cm^2}$, and the spatial resolution $\Delta x = \Delta y = 0.08$ cm. The scaling parameter α shown in Fig. 3 was used in the reconstruction. Figure 5(b) shows the fully scanned image, and (c), (d), and (e) are reconstructed images with acceleration factors of 2x, 3x, and 4x, respectively. Even though aliasing artifacts remained on the images, high-resolution images were obtained even for an acceleration factor of 4x, as shown in Fig 5(e).

VI. Discussion

Let the acceleration factor be X_a, then the fold-over artifacts appear at every $1/X_a$ of FOV in the scaled space, as shown in Figs. 3(a), 3(b), and 3(c). This distance is similar to the fold-over artifacts in the reconstructed images in standard Fourier transform imaging. However, the scale of the reconstructed images is much smaller than standard Fourier-transform-based images, and the main image and aliased image components are separated in the scaled space. Therefore, it is feasible to reduce the aliasing artifacts by removing the alias-dominant components. In general, it is difficult to separate the aliased image components in any space in standard Fourier-transform-based imaging, and proposed alias control has significant advantages over other reconstruction methods. This is the major reason why the proposed method has a higher PSNR than other methods, as shown in Fig. 4. Second, it is not necessary to acquire the signal continuously in k-space central, as in standard k-space undersampling, and the signal compression ratio will be increased. Third, the obtained images are not severely sacrificed by undersampling because equi-space sampling is performed instead of random undersampling. Recently, several papers have used regular undersampling in the application of CNN to CS[18], [19]. Regular undersampling has advantages such that blurring of the reconstructed image is smaller compared to random undersampling, especially for lower sampling rates. Previous studies have pointed out that it is easier for the CNN to learn the rule of the fold-over effect in regular undersampling than in random undersampling because the manner of aliasing that occurs is very simple and easy to recognize. The results shown in Figs. 3 and 5(a) are consistent with these reports.

VII. Conclusion

A new fast imaging method using the equi-spaced undersampled PSFT signal is proposed. The aliasing artifacts are separated from the main image component in the scaled space introduced by aliasless image reconstruction. The aliasing artifacts are first reduced in the scaled space, and the remaining aliases are then removed using the image domain deep CNN. Reconstruction experiments show superior PSNR compared to ADMM-CSnet, image domain CNN, and conventional iterative reconstruction.

Acknowledgment

The present study was supported by JSPS KAKENHI 19K04423 and the Kayamori Foundation of Informational Science Advancement. The authors would like to thank Canon Medical Systems Corp. for the use of clinical magnetic resonance images.

References

[1] Donoho DL, “Compressed sensing,” IEEE Transactions on Information Theory, vol. 52, pp.1289-1306, 2006.

[2] Candès EJ, Romberg J, Tao T et al., "An Introduction To Compressive Sampling," IEEE Signal Processing Magazine, vol. 25, pp.21-30, 2008.
[3] Lustig M, Donoho D, Pauly JM, "Sparse MRI: The Application of Compressed Sensing for Rapid MR Imaging," Magn Reson Med, vol. 58, pp.1182–1195, 2007.
[4] Kwon K, Kim D, Park H, "A parallel MR imaging method using multilayer perceptron," Med. Phys, vol. 44, pp.6209-6224, 2017.
[5] Lee D, Yoo J, Tak S et al., "Deep Residual Learning for Accelerated MRI Using Magnitude and Phase Networks," IEEE Trans. Biomed. Eng, vol. 65, pp.1985-1995, 2018.
[6] Zhu B, Liu JZ, Cauley SF et al., "Image reconstruction by domain-transform manifold learning," Nature, vol. 555, pp.487-492, 2018.
[7] Ito S, Yamada Y, "Alias-free image reconstruction using Fresnel transform in the phase-scrambling Fourier imaging technique," Magnetic Resonance in Medicine, vol.60, No.2, pp.422-430, 2008.
[8] Ito S, Yamada Y, "Reduction of Remained Artifacts in Alias-free Reconstruction of MR Images," International Society of Magnetic Resonance in Medicine 21th Scientific Meeting, Saltlake city, USA, 2675, 2013.
[9] Yang Y, Sun J, Li H et al., "ADMM-CSNet: A Deep Learning Approach for Image Compressive Sensing," IEEE Tran PAMI, doi: 10.1109/TPAMI.2018.2883941.
[10] Maudsley A A, "Dynamic range improvement in NMR imaging using phase scrambling," Journal of Magnetic Resonance Imaging, vol.76, pp. 287–305, 1988.
[11] Wedeen VJ, Chao YS, Ackerman JL, "Dynamic Range Comp-pression in MRI by Means of a Nonlinear Gradient Pulse," Magn Reson Med, vol.6, pp. 287–295, 1988
[12] Yamada Y, Tanaka K, Abe Z, "NMR Fresnel transform imaging technique using a quadratic nonlinear field gradient," Rev. Sci. Instrum.,vol.63, no.11, pp.5349–5358, 1992.
[13] Stockman JP, Ciris PA, Galiana G et al., "O-space images: highly efficient parallel imaging using second-order nonlinear fields as encoding gradients," Magnetic Resonance in Medicine, vol.64, No.2, pp.447-456, 2010.
[14] Dispenza NL, Littin S, Zaitev M, et al., "Clinical Potential of a New Approach to MRI Acceleration," Scientific Reports, vol.9, 1912, 2019.
[15] Wang H, Tam LK, Constable RT, Galiana G. Fast rotary nonlinear spatial acquisition(FRONSAC) imaging. Magn Reson Med. vol.75, pp.1154?1165, 2016
[16] Zhang K, Zuo W, Chen Y et al., "Beyond a Gaussian Denoiser: Residual Learning of Deep CNN for Image Denoising," IEEE Trans on Image Proc, vol. 26, pp.3142-3155, 2017.
[17] Wiaux Y, Puy G, Gruetter R, et al., "Spread Spectrum for Compressed Sensing Techniques in Magnetic Resonance Imaging," IEEE ISBI, pp.756–759, Rotterdam, The Netherlands, 2010.
[18] Hammernik K, Knoll F, Sodickson D et al., "On the influence of Sampling Pattern Design on Deep Learning-Based MRI Reconstruction," International Society of Magnetic Resonance in Medicine, O644, Hawaii, 2018.
[19] Hyun CM, Kim HP, Lee SM, et al., "Deep learning for undersampled MRI reconstruction," Physics in Medicine and Biology, vol. 63, no.13, 135007(15pp), 2018.